

Applicability of the cubic model to the critical behavior of real systems*

D. Kim,[†] P. M. Levy,[‡] and J. J. Sudano[‡]

Department of Physics, New York University, 4 Washington Place, New York, New York 10003

(Received 21 July 1975)

We have previously developed a model Hamiltonian called the cubic model to explain the salient features of the critical behavior of a group of cubic rare-earth compounds. There are interaction terms present in real systems that were neglected in this model. Here we consider how they modify the tricritical-like phase transition of the cubic model that was predicted by using the mean-field approximation. We find that for rare-earth compounds with large angular momentum J , the neglect of the overlap between the sixfold degenerate states is justified. Crystal fields which make a nonmagnetic state lowest in energy tend to drive the transition first order. These results which are readily obtained only within the mean-field approximation are expected to hold in better statistical approximations. Within both the mean-field and Bethe-Peierls-Weiss approximation quadrupolar pair interactions that favor parallel ordering of the moments drive the transition first order, while those favoring perpendicular ordering of the moments drive the transition second order. As the cubic model has a first-order phase transition in the Bethe-Peierls-Weiss approximation in zero fields, the transition is not tricritical. Therefore we have determined by using this approximation the size of the single-ion anisotropy, or quadrupolar pair interaction, needed to drive the system tricritical. The magnitudes required to achieve this are within the limits estimated from experimental data.

I. INTRODUCTION

The cubic model¹ was recently introduced to explain the tricritical-like behavior of cubic rare-earth compounds, in particular holmium antimonide, HoSb. The Hamiltonian for this model is given as

$$\mathcal{H} = -J \sum_{\langle ij \rangle} \sigma_i \sigma_j \delta_{\alpha_i \alpha_j}, \quad (1)$$

where σ takes on the values ± 1 and α the values x , y , and z . To arrive at this model we made several approximations; we neglected the overlap between the eigenstates that point along different cube axes, we assumed the crystal field was such as to cause the lowest six levels to be degenerate, and we neglected the quadrupolar pair interactions that are present in real systems. In this paper we determine the effects of including these terms on the thermodynamic behavior of the cubic model.

When we include the crystal field and nonorthogonality of the basis states we have a matrix representation of the Hamiltonian which is *nondiagonal*. In the mean-field approximation (MFA) we can readily deal with the nondiagonal matrices and determine the effects of these terms by *analytic* solutions. Although we know that certain features of the cubic model as determined by the mean-field approximation are incorrect,² we have not undertaken the lengthy Bethe-Peierls-Weiss (BPW) calculation, which provides only numerical solutions, because the crystal field parameters are not known for the system of particular interest to us HoSb. Including quadrupolar interactions does

not lead to nondiagonal matrices and for this reason we are readily able to determine the effects of this additional term on the behavior of the cubic model in the BPW approximation. However, the MFA calculation is also presented because the analytic solutions obtained give us a clearer insight into the effect these interactions have on the critical behavior of the cubic model.

In Secs. II, III, and IV we determine within the mean-field approximation how these additional terms affect the nature of the phase transition, i.e., whether it is first order, second order, or tricritical-like. If we include the overlap of the eigenstates we find that the phase transition for the cubic model asymptotically approaches second-order behavior. However, for HoSb one must be extremely close to T_c to see this behavior, i.e., $t = (T_c - T)/T_c < 10^{-3}$. The effect of crystal fields which do not produce sixfold degenerate ground states is to drive the tricritical-like phase transition of the cubic model discontinuous, i.e., first order. Depending on their sign the quadrupolar pair interactions can drive the transition either first order or second order. In Sec. V we have studied the thermodynamic behavior of our cubic model with quadrupolar pair interaction by using the Bethe-Peierls-Weiss approximation. As the phase transition of the cubic model is first order in this approximation we determine the magnitudes of the single-ion anisotropy and quadrupolar pair interaction that are needed to drive the cubic model tricritical. These magnitudes are quite reasonable in comparison to the estimates of bounds on these terms from experimental data.

From these studies we have obtained a better understanding of how the neglected terms and various approximations affect the predicted thermodynamic behavior of the cubic model. These results are needed to interpret and extract information from the existing experimental data on the rare-earth pnictides; particularly on HoSb. However, the lack of sufficient data on the crystal field parameters and the size of the quadrupolar pair interactions in HoSb precludes us from making a definitive analysis of the thermodynamic behavior of the compound at the present time.

II. NONORTHOGONALITY

In deriving the cubic model, we neglected the overlap between states quantized along different cube axes

$$\langle \pm q | \pm q' \rangle = 2^{-J} \equiv \Delta \quad (2)$$

where $|\pm q\rangle \equiv |J \pm J\rangle_q$, $q, q' = x, y, z$, and $q \neq q'$. Let us now include this overlap and determine the thermodynamic properties of the model. Wherever we must be specific, we consider the case of Ho^{3+} ($J=8$) in HoSb. Written in the basis of the states $|\pm q\rangle$, the angular momentum operator S_z , see Eq. (7) of I, is

$$S_z = \begin{pmatrix} 0 & 0 & -i\Delta & i\Delta & \Delta & -\Delta \\ 0 & 0 & i\Delta & -i\Delta & \Delta & -\Delta \\ i\Delta & -i\Delta & 0 & 0 & \Delta & -\Delta \\ -i\Delta & i\Delta & 0 & 0 & \Delta & -\Delta \\ \Delta & \Delta & \Delta & \Delta & 1 & 0 \\ -\Delta & -\Delta & -\Delta & -\Delta & 0 & -1 \end{pmatrix}. \quad (3)$$

The matrices for S_x and S_y are the appropriate permutations of S_z . In this same representation the identity matrix is

$$I = \begin{pmatrix} 1 & 0 & \Delta & \Delta & \Delta & \Delta \\ 0 & 1 & \Delta & \Delta & \Delta & \Delta \\ \Delta & \Delta & 1 & 0 & \Delta & \Delta \\ \Delta & \Delta & 0 & 1 & \Delta & \Delta \\ \Delta & \Delta & \Delta & \Delta & 1 & 0 \\ \Delta & \Delta & \Delta & \Delta & 0 & 1 \end{pmatrix}. \quad (4)$$

We note that the overlap Δ causes the angular momentum and identity matrices to be nondiagonal. Also the eigenvalue problem for the mean-field Hamiltonian is in a nonorthogonal basis $\mathcal{H} - \lambda I = 0$.

To simplify these calculations we construct a set of orthonormal states from the basis $|\pm q\rangle$ that transform according to the irreducible representation of the cubic group. For Ho^{3+} ($J=8$) these functions are given by Trammell as³

$$\begin{aligned} |\Gamma_1\rangle &= (1/\sqrt{6\beta})(|z\rangle + |-z\rangle + |x\rangle + |-x\rangle + |y\rangle + |-y\rangle), \\ |\Gamma_{31}\rangle &= (1/\sqrt{3\alpha})(|z\rangle + |-z\rangle - \frac{1}{2}(|x\rangle + |-x\rangle + |y\rangle + |-y\rangle)), \\ |\Gamma_{32}\rangle &= (1/\sqrt{4\alpha})(|x\rangle + |-x\rangle - |y\rangle - |-y\rangle), \\ |\Gamma_{41}\rangle &= (1/\sqrt{2})(|z\rangle - |-z\rangle), \\ |\Gamma_{42}\rangle &= (1/\sqrt{2})(|x\rangle - |-x\rangle), \\ |\Gamma_{43}\rangle &= (1/\sqrt{2})(|y\rangle - |-y\rangle), \end{aligned} \quad (5)$$

where $\alpha \equiv 1 - 2\Delta$ and $\beta \equiv 1 + 4\Delta$.

The Hamiltonian which represents the pair interactions in our model is

$$\mathcal{H} = - \sum_{\langle ij \rangle} \mathcal{J}'_{ij} \vec{J}_i \cdot \vec{J}_j. \quad (6)$$

In the mean-field approximation this reduces to

$$\mathcal{H}_{\text{MFA}} = -I_{10} M J_z, \quad (7)$$

where $M \equiv \langle J_z \rangle$. As we are interested in only the low-temperature behavior of HoSb, we project this Hamiltonian on the ground-state manifold described by the states $|\Gamma_i\rangle$ in Eq. (5). Then, in the MFA our problem reduces to finding the eigenvalues of the matrix

$$-(1/kT)\mathcal{H}_{\text{MFA}} = \begin{pmatrix} 0 & 0 & 0 & 0 & 0 & 0 \\ 0 & 0 & -2i\Delta y & 0 & 0 & 0 \\ 0 & 2i\Delta y & 0 & 0 & 0 & 0 \\ 0 & 0 & 0 & 0 & (2\alpha/3)^{1/2}y & 0 \\ 0 & 0 & 0 & (2\alpha/3)^{1/2}y & 0 & (\beta/3)^{1/2}y \\ 0 & 0 & 0 & 0 & (\beta/3)^{1/2}y & 0 \end{pmatrix}, \quad (8)$$

where

$$y \equiv 8I_{10}M/kT = m/\bar{T},$$

$$m \equiv \frac{1}{8} \langle J_z \rangle,$$

and

$$\bar{T} \equiv kT/64I_{10}. \quad (9)$$

To arrive at this matrix we rearranged the ordering of the states given in Eq. (5). The eigenvalues of this matrix are 0, $\pm y$, and $\pm 2\Delta y$, and the partition function is

$$Z_{\text{MFA}} = 2 + 2 \cosh y + 2 \cosh 2\Delta y. \quad (10)$$

With this partition function the self consistent equation for the magnetization is given as

$$m = (2\Delta \sinh 2\Delta y + \sinh y)/(1 + \cosh 2\Delta y + \cosh y) \quad (11)$$

$$= \left[\frac{1}{3}(1 + 4\Delta^2) \right] y - \frac{4}{9} \Delta^2 y^3 - \frac{1}{540} (1 - 30\Delta^2 - 120\Delta^4 + 64\Delta^6) y^5 + \dots \quad (12)$$

In the presence of a magnetic field H along the Z axis, the variable y becomes

$$y = (m + \tilde{H})/\bar{T}, \quad (13)$$

where

$$\tilde{H} \equiv g\mu_B H/8I_{10}.$$

Upon placing this into Eq. (12) we find the equation of state is

$$\tilde{H}/\bar{T} = \left[3/(1 + 4\Delta^2) - 1/\bar{T} \right] m + \left[36\Delta^2/(1 + 4\Delta^2) \right] m^3 + \dots \quad (14)$$

This implies that in zero external field, $\tilde{H}=0$, the transition is of the second order at

$$\bar{T}_c = \frac{1}{3}(1 + 4\Delta^2). \quad (15)$$

If we set $\Delta=0$ in Eqs. (14) and (15), i.e., neglect overlap or nonorthogonality of the basis states, we recover the results obtained for the cubic model, i.e., a phase transition at $\bar{T}_c = \frac{1}{3}$ with tricritical-like critical exponents. At first sight, it seems that overlap, i.e., finite Δ , produces a qualitative difference in the phase transition. However, the coefficient of the m^3 term, $36\Delta^2 \sim 5.5 \times 10^{-4}$, is very small for Ho^{3+} ($J=8$), and the behavior of the system, e.g., the magnetization Eq. (11), will be tricritical-like except for temperatures T very close to T_c . This is illustrated in Fig. 1 by the log-log plot of the spontaneous magnetization for the two cases. From this plot we see that for reduced temperatures $t = (T_c - T)/T_c$ greater than 10^{-4} , which is the region accessible to experimental study, the two cases ($\Delta=0$ and $\Delta \neq 0$) are indistinguishable with an effective critical exponent β of $\frac{1}{4}$. The truly asymptotic behavior with $\beta = \frac{1}{2}$ sets in only for $t \lesssim 10^{-8}$.

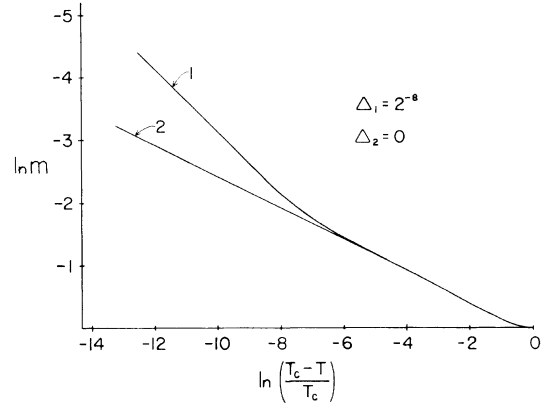


FIG. 1. A log-log plot of the magnetization versus the reduced temperature $t \equiv (T_c - T)/T_c$ of the cubic model. Curve 1: When the overlap between the degenerate states is taken into account and the slope β is asymptotically $\frac{1}{2}$. We choose $\Delta = 2^{-8}$ the overlap appropriate for Ho^{3+} , $J=8$. Curve 2: When overlap is neglected, and the slope $\beta = \frac{1}{4}$.

We conclude that for holmium compounds ($J=8$) the neglect of the overlap in the basis states does not produce any *observable* differences in the thermodynamic behavior of these compounds. However, for rare earths with smaller angular momentum the overlap increases because $\Delta = 2^{-J}$. Then the coefficient of m^3 , $36 \times 2^{-2J} \cong 2^{5-2J}$, may be sufficiently large to produce discernable differences in the thermodynamic behavior of these compounds. Although these results were obtained on the basis of the MFA we do not expect them to differ in better approximations.

III. CRYSTAL FIELD

The cubic model Eq. (1) was derived by projecting an isotropic pair interaction on the sixfold degenerate ground-state manifolds of rare-earth ions.¹ For these manifolds to be sixfold degenerate the cubic crystal field parameters as defined by Lea, Leask, and Wolf⁴

$$V_c = B_4 O_4 + B_6 O_6, \quad (16)$$

must assume a specific ratio B_4/B_6 , that is to say, the parameter X which is related to B_4/B_6 must take on a value X_c such that the cubic crystal field leaves the ground-state manifold sixfold degenerate. In real systems one does not expect the crystal fields to be exactly at this propitious value of X ; however, they may have ratios X close to X_c . For example, for HoSb we estimate $X = 0.67$ while $X_c = \frac{6}{7} = 0.85$. Therefore in this section we study how the nature of the phase transition of the cubic model changes when the crystal field has ratios X not equal to, but close to, X_c .

The effects of a crystal field with $X \neq X_c$ are twofold. First it splits the sixfold degenerate ground state manifold into a singlet, doublet, and triplet. Secondly, the field admixes the upper excited states into the ground states given by Eqs. (5). Trammell³ has found that for ratios of the crystal field parameters close to X_c one can obtain good estimates of the splittings of the ground-state energy levels without taking into account the admixtures from the excited states. Therefore we first determine the effect of a crystal field on the phase transitions of our model by neglecting admixtures from excited states. Then we include admixtures in the basis states caused by a crystal field with $X \neq X_c$ and find how this affects the critical behavior of our model. In our calculations we explicitly consider Ho^{3+} , however our results will be applicable to other rare earths.

In the sixfold manifold of states given by Eq. (5) the cubic crystal field given by Eq. (16) is diagonal

$$V_c = 60B_4a_1\mathcal{G} + W \begin{bmatrix} -4/\beta & & & & & \\ & 2/\alpha & & & & \\ & & 2/\alpha & & & \\ & & & 0 & & \\ & & & & 0 & \\ & & & & & 0 \end{bmatrix}, \quad (17)$$

$$-\frac{1}{kT} \mathcal{H}_{\text{MFA}} = \begin{bmatrix} -2a/\alpha & 0 & 0 & 0 & 0 & 0 \\ 0 & 0 & -2i\Delta y & 0 & 0 & 0 \\ 0 & 2i\Delta y & 0 & 0 & 0 & 0 \\ 0 & 0 & 0 & -2a/\alpha & (2\alpha/3)^{1/2}y & 0 \\ 0 & 0 & 0 & (2\alpha/3)^{1/2}y & 0 & (\beta/3)^{1/2}y \\ 0 & 0 & 0 & 0 & (\beta/3)^{1/2}y & 4a/\beta \end{bmatrix}, \quad (18)$$

where $a \equiv W/kT \equiv \bar{W}/\bar{T}$, $\bar{W} \equiv W/64I_{10}$, and y and \bar{T} are defined by Eq. (9). The eigenvalues of this matrix are $-2a/\alpha$, $\pm 2\Delta y$, and the three roots E_i ($i=1, 2, 3$) of the following cubic equation:

$$E^3 - \frac{2\gamma}{\alpha\beta} aE^2 - \left(\frac{8}{\alpha\beta} a^2 + y^2\right)E + \frac{2\gamma}{\alpha\beta} ay^2 = 0, \quad (19)$$

where $\gamma \equiv 1 - 8\Delta$. The partition function in the MFA is

where α and β are defined in Eqs. (5),

$$\begin{aligned} a_1 &\equiv 364(1 + 66B_6/B_4), \\ W &\equiv (6825/16)B_4(1386B_6/B_4 - 1) \\ &= (6825/16)B_4(6/X - 7), \\ X &= (231B_6/B_4 + 1)^{-1}, \end{aligned}$$

and \mathcal{G} represents the unit matrix. Here the parameter X is that used by Lea, Leask, and Wolf⁴; however, our W is *not* the one used by them. When the ratio of the crystal field parameters is such that $X = X_c = \frac{6}{7}$, $W = 0$, and the second term in Eq. (17) is zero. For $X \neq X_c$ the crystal field splits the ground manifold into a singlet Γ_1 , a doublet Γ_3 , and a triplet Γ_4 . As B_4 is negative for HoSb , the coefficient W is negative when $X < X_c$ and the Γ_3 doublet state lies lowest; for $X > X_c$, W is positive and the Γ_1 singlet is lowest in energy.

The Hamiltonian for our system now consists of the crystal field Eq. (17) and the pair interaction Eq. (6). As the first term in the crystal field Eq. (17) only shifts the energy scale we will neglect this constant term from here on in. In the mean-field approximation, the determination of the partition function reduces to finding the eigenvalues of the Hamiltonian consisting of the second term of Eq. (17) and the mean-field approximation to the pair interaction Eq. (7). After rearranging the rows and columns of this matrix we find

$$Z_{\text{MFA}} = e^{-2a/\alpha} + 2 \cosh 2\Delta y + \sum_{i=1}^3 e^{E_i(y,a)}, \quad (20)$$

and the free energy is given as

$$-F/kT = -\bar{F}/\bar{T} = \ln Z_{\text{MFA}} - m^2/2\bar{T}, \quad (21)$$

where $\bar{F} \equiv F/64I_{10}$. From this we find the equation of state is

$$m = Z_{\text{MFA}}^{-1} \left(4\Delta \sinh 2\Delta y + \sum_{i=1}^3 E'_i e^{E_i} \right), \quad (22)$$

where

$$E'_i = \frac{2\gamma[E_i - (2\gamma/\alpha\beta)a]}{3E_i^2 - (4\gamma/\alpha\beta)aE_i - (8a^2/\alpha\beta + \gamma^2)}.$$

This equation must be solved self consistently for m as a function of T and H .

We have solved Eqs. (20), (21), and (22) and we find the phase diagram in $\tilde{T} - \tilde{W}$ space shown in Fig. 2. For \tilde{W} near zero there is a small line of second-order phase transitions. This line is parametrically described by the equations

$$\tilde{T}_c = \frac{8\Delta^2 + \gamma/2a - (2\alpha^2/3a)e^{-2a/\alpha} + (\beta^2/6a)e^{4a/B}}{3 + 2e^{-2a/\alpha} + e^{4a/B}}$$

and

$$\tilde{W} = a\tilde{T}_c \quad (23)$$

for $-0.00746 \leq a \leq 0.113$, or $-0.00249 \leq \tilde{W} \leq 0.0372$. For this range of \tilde{W} , the critical temperatures are explicitly given as

$$T_c = \frac{1}{3}(1 + 4\Delta^2) + (4\Delta/\alpha\beta)\tilde{W} - 2[(1 - 4\Delta + 52\Delta^2 + 96\Delta^4)/\alpha^2\beta^2(1 + 4\Delta^2)^2]\tilde{W}^2 + \dots \quad (24)$$

The first-order portion of the phase diagram has been determined numerically. As the lowest states for all values of \tilde{W} are nonmagnetic, either Γ_3 or Γ_1 , there are no phase transitions for $\tilde{W} > \tilde{W}_1 = 0.176$ and for $\tilde{W} < \tilde{W}_2 = \frac{1}{3}(-2\alpha^2) \cong -\frac{2}{3}$. In Fig. 2 we have also shown the line representing the stability limit of the high-temperature phase. This line is the continuation of Eq. (23) for \tilde{W} where the transition is first order.

We have also determined as a function of the

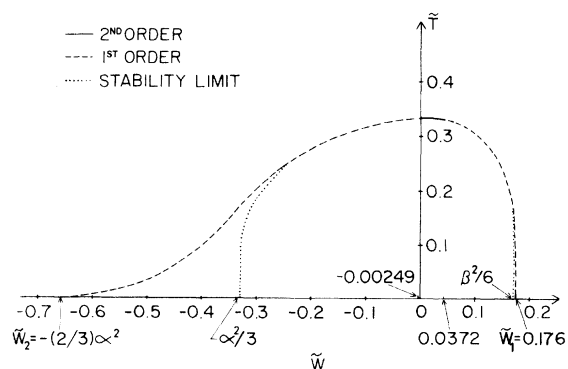


FIG. 2. Phase diagram in $\tilde{T} - \tilde{W}$ space which depicts the effect of cubic crystal fields on the critical behavior of the cubic model. The solid line, about $\tilde{W} = 0$, represents the region for which one has second-order phase transitions. First-order phase transitions are denoted by the dashed lines. The stability limit of the high-temperature phase is denoted by the dotted lines.

crystal field parameter \tilde{W} the discontinuity in the order parameter at T_c , Δm , and the saturation moment at $T = 0^\circ\text{K}$, m_s . These variations are shown in Fig. 3. For $\tilde{W} > \tilde{W}_1$ the $m_s = 0$; but at $\tilde{W} = \tilde{W}_1$ the saturation moment suddenly jumps to $m_{s0} = 0.509$. Near $\tilde{W} = 0$ the saturation moment is given as

$$m_s \cong 1 - (4/\alpha\beta)\tilde{W}^2 - (16\gamma/\alpha^2\beta^2)\tilde{W}^3 + \dots \quad (25)$$

As \tilde{W} approaches \tilde{W}_2 , m_s vanishes quadratically. In Fig. 2, it is particularly interesting to note that for $-0.25 \leq \tilde{W} \leq 0.16$ the coexistence and stability curves *nearly* overlap, i.e., $(T_c - T_0)/T_c \cong 10^{-3}$ for $\tilde{W} \sim -0.2$ where T_0 is the stability limit. From Fig. 3 we see that in this region discontinuity of the order parameter is quite sizeable. Therefore for real systems with \tilde{W} in this region one should observe a discontinuity of the order parameter and an apparent divergence of the susceptibility.⁵

The crystal field parameters for real systems as HoSb are not known. When we use the values of B_4 and B_6 obtained from the linear interpolation between those of PrSb and TmSb,⁶ we find $X = 0.67$ and $\tilde{W}/\tilde{T}_c \sim -\frac{1}{2}$. On the basis of our results in Figs. 2 and 3, HoSb should experience a discontinuous transition but with a susceptibility that appears to diverge.

Now we will take into account the admixtures of excited states in the wave functions of the ground state caused by crystal fields with $W \neq 0$. We take $X = 0.67$, the estimated value for HoSb, and we obtain the correct wave functions by interpolating between those given by Lea, Leask, and Wolf.⁴ The mean field Hamiltonian Eq. (18) evaluated in these states is

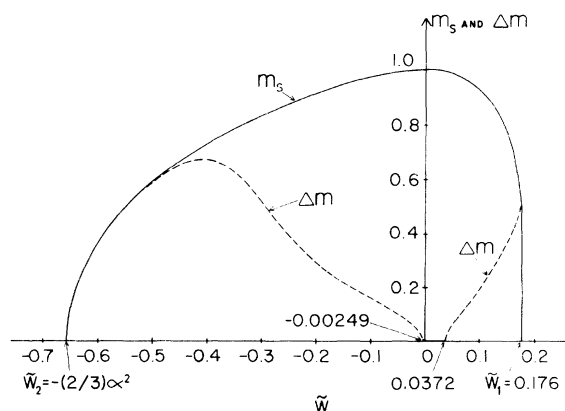


FIG. 3. Jump in the spontaneous magnetization at the transition temperature Δm and the saturation magnetization at $T = 0^\circ\text{K}$, m_s as a function of the crystal field parameter \tilde{W} . At the threshold $\tilde{W}_1 = 0.176$, $m_s = \Delta m = 0.509$.

$$-\frac{1}{kT} \mathcal{K}_{\text{MFA}} = \begin{bmatrix} -2a' & 0 & 0 & 0 & 0 & 0 \\ 0 & 0 & -iDy & 0 & 0 & 0 \\ 0 & iDy & 0 & 0 & 0 & 0 \\ 0 & 0 & 0 & -2a' & Ey & 0 \\ 0 & 0 & 0 & Ey & 0 & Fy \\ 0 & 0 & 0 & 0 & Fy & 4\eta a' \end{bmatrix}, \quad (26)$$

where

$$D=0.057, \quad E=0.82, \quad F=0.54, \quad \eta=1.17,$$

and $a' \equiv W'/kT = \bar{W}'/\bar{T}$. The parameter W' is determined by evaluating the crystal field Hamiltonian Eq. (16) in the set of six states appropriate to HoSb, i.e., $X=0.67$. By using the interpolated values of the parameters B_4 and B_6 we find $W' = -2.25^\circ\text{K}$ for HoSb. However, we will treat W' as a parameter, so as to ascertain the effect of varying B_4 and B_6 on the nature of the phase transition.

We proceed as before to find the eigenvalues of Eq. (26) and then the partition function and free energy. We find that the phase diagram in $\bar{T} - \bar{W}'$ space is qualitatively similar to the one shown in Fig. 2 but with $\bar{W}'_1=0.125$, $\bar{W}'_2=-0.676$, and $\bar{T}_c(\bar{W}'=0)=0.324$. The major difference is that the critical line extends over a larger range of \bar{W}' ;

$$-0.214 < \bar{W}' < 0.018.$$

For HoSb, with $W' = -2.25^\circ\text{K}$ and $T_c = 5.4^\circ\text{K}$, we have $a' = -0.42$, or by using $I_{10} = 0.275^6$ we have $\bar{W}' = -0.13$ and $\bar{T}_c = 0.306$. For this value of \bar{W}' , the transition is second order. Therefore there are discernible differences in the phase transitions when we take account of the admixtures of excited states into the ground manifold states due to the crystal field. We conclude that in order to obtain an accurate description of the critical behavior of these cubic rare-earth compounds it is necessary to include these admixtures.

IV. QUADRUPOLE PAIR INTERACTIONS

In our previous paper (I) we have determined how quadrupolar pair interactions project onto the sixfold degenerate manifolds of the cubic model. Although in our previous work we separately considered bilinear and quadrupolar pair interactions, now we will consider them simultaneously.

In this section we use the MFA to obtain analytic solutions for the thermodynamic behavior of the cubic model with quadrupolar pair interactions. Better quantitative results are obtained in the following section by using the BPW approximation.

The Hamiltonian which represents the cubic model with isotropic quadrupolar pair interactions is given as

$$\mathcal{K} = -\mathcal{J} \sum_{\langle ij \rangle} \mathfrak{S}_i \cdot \mathfrak{S}_j - \eta \mathcal{J} \sum_{\langle ij \rangle} \left[\left(\frac{3\mathfrak{S}_{z_i}^2 - 1}{2\sqrt{3}} \right) \left(\frac{3\mathfrak{S}_{z_j}^2 - 1}{2\sqrt{3}} \right) + \frac{1}{4} (\mathfrak{S}_{x_i}^2 - \mathfrak{S}_{y_i}^2) (\mathfrak{S}_{x_j}^2 - \mathfrak{S}_{y_j}^2) \right] - \bar{H} \cdot \sum_i \mathfrak{S}_i - D_1 \sum_i \left(\frac{3\mathfrak{S}_{z_i}^2 - 1}{2\sqrt{3}} \right) - \frac{1}{2} D_2 \sum_i (\mathfrak{S}_{x_i}^2 - \mathfrak{S}_{y_i}^2), \quad (27)$$

where the i and j go over the $\frac{1}{2}zN$ nearest-neighbor pairs and we have written the quadrupolar coupling as $\mathcal{K} \equiv \eta \mathcal{J}$. The spin matrices \mathfrak{S}_q are given by Eq. (3) with the overlap set to zero, $\Delta = 0$. The absence of the terms like $\mathfrak{S}_x \mathfrak{S}_y$ in the quadrupolar pair interactions can be seen from their matrix representations

$$\mathfrak{S}_x \mathfrak{S}_y = \begin{bmatrix} 1 & & & & & \\ & -1 & & & & \\ & & 0 & & & \\ & & & 0 & & \\ & & & & 0 & \\ & & & & & 0 \end{bmatrix} \begin{bmatrix} 0 & & & & & \\ & 0 & & & & \\ & & 1 & & & \\ & & & -1 & & \\ & & & & 0 & \\ & & & & & 0 \end{bmatrix} = 0.$$

The symmetry properties of the free energy in the complete field space (\bar{H}, \bar{D}, T) as discussed in I Sec. III, all remain valid in the presence of quadrupolar pair interactions, i.e., for the system described by Eq. (27).

We now proceed to determine the effects of quadrupolar pair interactions on the critical behavior of the cubic model. As this model is defined with $\eta = 0$, we will be interested in this behavior of the model Hamiltonian Eq. (27) for small values of η . Also, we will be interested in negative as well as positive values of η . If η becomes sufficiently negative for $\mathcal{J} > 0$, one finds that the system does not order in a ferromagnetic, ferroquadrupolar array; the negative η prefers a perpendicular or antiferroquadrupolar ordering of the quadrupolar moments. In our work we will

always consider η sufficiently small so that one maintains ferromagnetic ordering.

In applying the MFA to our model Eq. (27) we proceed as in I (Sec. IV) and we find the reduced free energy is

$$f = T \sum_{\alpha=1}^6 \rho_{\alpha} \ln \rho_{\alpha} - \frac{1}{2} \vec{M} \cdot \vec{M} - \frac{1}{2} \eta (Q_1^2 + Q_2^2) - \vec{H} \cdot \vec{M} - \vec{D} \cdot \vec{Q}, \quad (28)$$

where the energies are in units of $I \equiv zJ$, T means kT/I , and all other quantities are defined in I. The only difference between the free energy of the cubic model Eq. (32) of I and Eq. (28) is the extra term $-\frac{1}{2} \eta \vec{Q} \cdot \vec{Q} \equiv -\frac{1}{2} \eta (Q_1^2 + Q_2^2)$. Consequently, the equations of state that result from the self consistency conditions are

$$\begin{aligned} \frac{1}{6} + Q_1/\sqrt{3} \pm \frac{1}{2} M_3 &= \alpha \exp\{[\pm M_3 \pm H_3 + (\frac{1}{2}\sqrt{3})(\eta Q_1 + D_1)]/T\}, \\ \frac{1}{6} - (1/2\sqrt{3})Q_1 + \frac{1}{2} Q_2 \pm \frac{1}{2} M_1 &= \alpha \exp\{[\pm M_1 \pm H_1 + \frac{1}{2}(\eta Q_2 + D_2)]/T\}, \\ \frac{1}{6} - (1/2\sqrt{3})Q_1 - \frac{1}{2} Q_2 \pm \frac{1}{2} M_2 &= \alpha \exp\{[\pm M_2 \pm H_2 - \frac{1}{2}(\eta Q_2 + D_2)]/T\}, \end{aligned} \quad (29)$$

where

$$\begin{aligned} \alpha^{-1} &= 2e^{\sqrt{3}(\eta Q_1 + D_1)/2T} \cosh[(M_3 + H_3)/T] \\ &+ 2e^{(\eta Q_2 + D_2)/2T} \cosh[(M_1 + H_1)/T] \\ &+ 2e^{-(\eta Q_2 + D_2)/2T} \cosh[(M_2 + H_2)/T]. \end{aligned} \quad (30)$$

These equations parallel those given in I with the modification that D_{α} goes into $D_{\alpha} + \eta Q_{\alpha}$ when we consider quadrupolar interactions.

From now on we consider only the zero field $\vec{H} = \vec{D} = 0$ case, and we approach this limit as $D_1 \rightarrow 0^+$, $H_3 \rightarrow 0^+$, for $H_1 = H_2 = 0$ and $D_2 = 0$. In this case we may assume that the ordering whenever present is along the z -direction, i.e., $M_3 \geq 0$, $Q_1 \geq 0$, $M_1 = M_2 = Q_2 = 0$, and Eqs. (29) reduce to

$$\begin{aligned} M_3 &= \sinh x / (\cosh x + 2e^{-y}) \\ (2/\sqrt{3})Q_1 &= \cosh x / (\cosh x + 2e^{-y}) - \frac{1}{3}, \end{aligned} \quad (31)$$

where

$$x \equiv M_3/T$$

and

$$y \equiv (\frac{1}{2}\sqrt{3})\eta Q_1/T. \quad (32)$$

The trivial case $x = y = 0$ satisfies the above equations and is the solution with the lowest free ener-

gy for high temperatures.

To find the nontrivial solutions to Eqs. (31) and (32) we consider T and Q_1 as functions of M_3 . As these equations are even in M_3 we expand T and y as follows:

$$\begin{aligned} T &= T_0 + T_1 M_3^2 + O(M_3^4), \\ y &= y_0 + y_1 M_3^2 + O(M_3^4). \end{aligned} \quad (33)$$

We substitute these expansions into Eqs. (31) and (32) and equate the coefficients of equal powers of M_3 . From the first of the Eqs. (31) we find

$$T_0 = (2e^{-y_0} + 1)^{-1}, \quad (34a)$$

$$y_1(1 - T_0) = T_1/T_0 + 1/2T_0 - (1 - T_0)/12T_0^3, \quad (34b)$$

and from the second equation we find

$$T_0 = (\frac{4}{3}\eta)T_0 y_0 + \frac{1}{3}, \quad (34c)$$

$$(\frac{4}{3}\eta)(y_0 T_1 + T_0 y_1) = T_0(1 - T_0)(y_1 + 1/2T_0^2). \quad (34d)$$

By combining the first and third of these equations we find that y_0 is the solution of the following equation:

$$(2/\eta)y_0 = 1 - e^{-y_0}. \quad (35)$$

For $\eta > 2$ there are two solutions to this equation; the one with $y_0 \neq 0$ corresponds to that with lowest free energy and represents a quadrupolar phase with no dipolar moment $M_3 = 0$. As we are interested in small values of η we now confine our attention to $\eta < 2$. Then the only physical solution of Eq. (35) is $y_0 = 0$, and we find from Eqs. (34) that $T_0 = \frac{1}{3}$. In addition from Eqs. (34b) and (34d) we find

$$T_1 = (2/9)y_1 = \eta/(2 - \eta). \quad (36)$$

Consequently for $0 < \eta < 2$, it follows that $T_1 > 0$ and from Eqs. (33) that the curvature of the M_3 -vs- T plot is positive at T_0 . Therefore, the transition is discontinuous, i.e., first order, and takes place at some $T_c > T_0$. For $\eta < 0$, $T_1 < 0$ the curvature of M_3 versus T is negative and the transition is continuous, i.e., second order, at $T_c = T_0 = \frac{1}{3}$.

We conclude that the effect of a small quadrupolar pair interaction on the cubic model is to drive the phase transition first order when the interaction favors parallel alignment of the moments $\eta > 0$. If the quadrupolar pair interaction favors a perpendicular ordering of the moments $\eta < 0$, then it drives the phase transition second order. Although these results have been derived in this section by using the MFA, they are consistent with those we obtain in Sec. V by using the BPW approximation.

V. BETHE-PEIERLS-WEISS APPROXIMATION

We have previously determined that in the BPW approximation the cubic model has a first-order phase transition in zero field.² Now we use this approximation to determine the magnitudes of the single-ion anisotropies \vec{D} , and the quadrupole pair interaction \varkappa to drive the phase transition tricritical. The Hamiltonian for the cubic model in the presence of external fields and an isotropic quadrupolar pair interaction is given by Eq. (27). In I we noted that for the spin matrices \mathfrak{S}_i the quadrupolar pair interaction can be rewritten as

$$\mathfrak{H}_Q = -\left(\frac{1}{6}\eta\right)\mathfrak{J} \sum_{\langle ij \rangle} [3(\mathfrak{S}_i \cdot \mathfrak{S}_j)^2 - 1] \quad (37)$$

where, as before, $\eta \equiv \varkappa/\mathfrak{J}$, the ratio of quadrupolar to dipolar coupling. Thus, the Hamiltonian we use to calculate the partition function is

$$-\frac{1}{kT} \mathfrak{H} = K \sum_{\langle ij \rangle} [(\mathfrak{S}_i \cdot \mathfrak{S}_j) + \eta'(\mathfrak{S}_i \cdot \mathfrak{S}_j)^2] + \vec{H}' \cdot \sum_i \vec{\mathfrak{S}}_i + \sum_{i,\alpha} D'_\alpha \mathfrak{S}_{\alpha i}^2, \quad (38)$$

where $K \equiv \mathfrak{J}/kT$, $\eta' \equiv \frac{1}{2}\eta$, $H' = H/kT$, $D'_1 = D_2/2kT$, $D'_2 = -D'_1$, $D'_3 = \sqrt{3} D_1/2kT$ and α takes on the values 1, 2, 3 or x, y, z . We have dropped the constant terms that enter in the quadrupole pair interaction, see Eq. (37), and the single ion anisotropy term D_1 , see Eq. (27). The Hamiltonian Eq. (38) now resembles Eq. (3) of II when $n=3$ with the exception that we have a quadrupolar pair interaction. The determination of the values of the quadrupolar pair coupling η and the single-ion anisotropy D'_α needed to drive the cubic model tricritical in the BPW approximation is similar, albeit more complicated, to the calculation of Paper II. The details of this calculation are given in Appendix A.

In Fig. 4 we have plotted the solutions \vec{D}_t to Eq. (A12) for several values of η' . In particular we find the anisotropy fields \vec{D}_t necessary to drive the phase transition tricritical for a system, Eq. (27) or (38), with no quadrupolar pair interactions, $\eta'=0$. We have also found $\eta'_t = -0.046$ when $\vec{D} = 0$. In Fig. 5 we show the phase diagram for the cubic model with $\eta=0$, see Eq. (27), in $\vec{D}-T$ space, as determined by using the BPW approximation. The parameters in Fig. 5 refer to the Hamiltonian Eq. (27). This phase diagram differs from that found in the MFA (see Fig. 3 of I) in two respects. There is a region about the origin $\vec{D}=0$ in which the phase transition is first order. This region is bounded by the tricritical lines determined from Eq. (A12). The second difference is that the transition temperatures determined in the BPW approximation are lower than those determined by the MFA. In

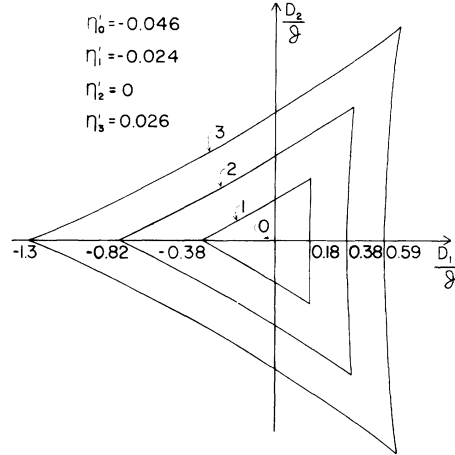


FIG. 4. Single-ion anisotropy fields \vec{D}_t necessary to drive the phase transition tricritical in the BPW approximation for a system described by Eq. (38). The various curves correspond to different values of the quadrupolar pair interaction constant η' . The points inside a curve represent first-order phase transitions; those outside a curve represent second-order phase transitions. In this figure the anisotropy fields \vec{D} are measured in units of the coupling constant \mathfrak{J} .

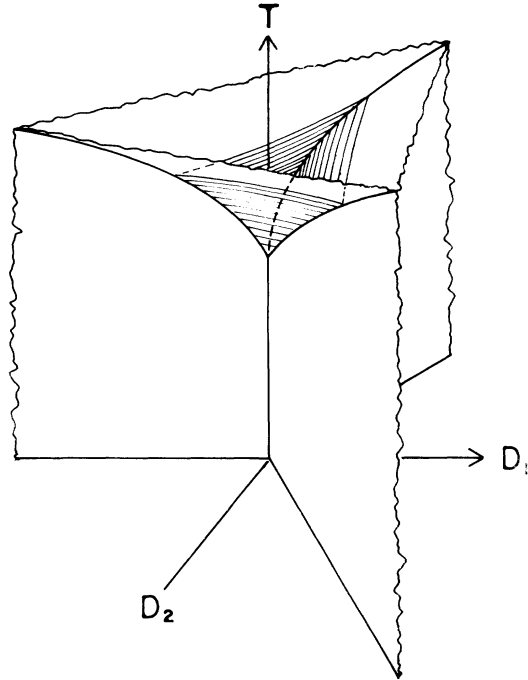


FIG. 5. Phase diagram for the cubic model Eq. (27) with $\eta=0$ in $\vec{D}-T$ space, as determined by using the BPW approximation. The region about the origin $\vec{D}=0$ corresponds to first-order phase transitions. Outside the line of tricritical points $\vec{D}=\vec{D}_t$, the transitions are second-order.

Fig. 6 we show a cross section of Fig. 5 with $D_2=0$, i.e., the variation of the transition temperature with single-ion anisotropy D_1 for the cubic model with $\eta=0$ in the BPW approximation. The phase diagram for the cubic model with $\eta=\eta_c \cong -0.1$ resembles Fig. 3 of I; only the transition temperatures are different.

The single-ion anisotropy fields needed to drive the system tricritical are small. In Appendix B we show that these fields can be produced by very small strains that may exist in cubic crystals. Similarly, the size of the quadrupolar pair interaction required to drive the system tricritical is not excessive. It is much smaller than the quadrupolar coupling found for HoSb by Mullen *et al.*⁷ from their analysis of the data on the softening of the elastic constant $C_{11} - C_{12}$. However, the sign of their coupling is such as to drive the model defined by Eq. (38) more first order. Therefore, either the effects due to a crystal field with $X \neq X_c$ which we neglected in Eq. (38) drive the transition tricritical, or a reanalysis of the data on the softening of the elastic constant ($C_{11} - C_{12}$) of HoSb based on better crystal field parameters and a better statistical mechanical approximation may yield a quadrupolar coupling which is negative $\eta' < 0$.

VI. DISCUSSION OF RESULTS

We introduced the cubic model to explain the unusual phase transition of HoSb. As real sys-

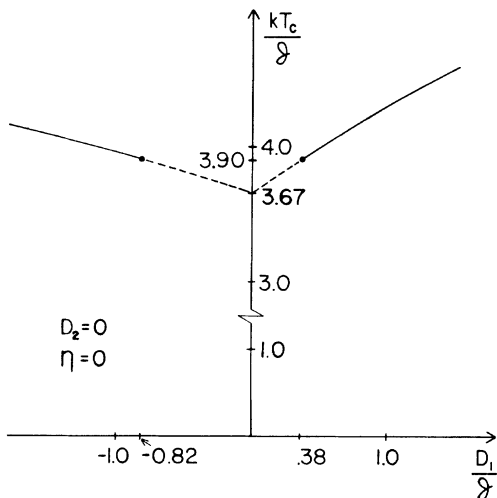


FIG. 6. Cross section of Fig. 5 with the single-ion anisotropy $D_2=0$. This shows the variation of the transition temperature with single-ion anisotropy D_1 for the cubic model with $\eta=0$ in the BPW approximation. In this figure the temperature and anisotropy are measured in terms of the coupling constant J . Solid lines represent second-order phase transitions, dashed lines represent first-order phase transitions.

tems do not satisfy all the conditions made in deriving this model we have studied how the neglected terms and approximations affect the nature of the phase transition of this model. From our results we conclude that it is reasonable to neglect the nonorthogonality of the six states that point along the cube axes. On the contrary, crystal fields which produce a splitting of the sixfold degenerate manifold of the cubic model and quadrupolar pair interaction do appreciably change the characteristics of the phase transition and should be included in calculations for real systems as HoSb. Also the BPW approximation rather than the MFA should be used to calculate the critical properties of the class of cubic rare-earth compounds described by the cubic model; although it provides analytic solutions the MFA does not give good quantitative results. Therefore, a realistic calculation of the thermodynamic behavior of the cubic rare-earth compounds requires that one use at least the BPW approximation *and* take into account the crystal fields and quadrupolar pair interactions.

The inclusion of the crystal field term in the Hamiltonian Eq. (27) or (38) leads to off diagonal terms in the cubic representation Eq. (2). The application of the BPW approximation to such a Hamiltonian is more complicated than the case encountered in Sec. V. As the crystal field parameters and quadrupolar pair interaction strengths (and sign) are not well known for HoSb, such a calculation cannot be undertaken at this time. However, by piecing together the results in Secs. III and V we conclude that when crystal fields are taken into account in a BPW calculation the size of the quadrupolar interaction needed to drive the system tricritical will be somewhat smaller. We can also consider how the results of a previous calculation,⁶ in which account was taken of the crystal field and quadrupolar interactions in the MFA, are modified when we use the BPW approximation. From the results in Sec. V we expect that the size of the quadrupolar pair interaction necessary to drive the system tricritical would be smaller than that found in the MFA. It might possibly be opposite in sign to that previously found.⁸

In conclusion, it will be necessary to obtain crystal field data (not interpolated parameters) and better estimates of the sign and size of the quadrupolar pair interaction for HoSb to more definitively ascertain whether our model explains the tricritical-like behavior of this system.

APPENDIX A: BETHE-PEIERLS-WEISS APPROXIMATION

The partition function for a cluster of spins which consists of a central ion and its q nearest neighbors is

$$Z_{cT} = 2^q \sum_{\alpha, \sigma} e^{H' \alpha \sigma + D' \alpha} \times \left[\sum_{\nu} e^{d_{\nu} + \eta' K \delta_{\alpha \nu}} \cosh(K \sigma \delta_{\alpha \nu} + h_{\nu}) \right]^q, \quad (\text{A1})$$

where $\sigma = \pm 1$, $\alpha, \nu = 1, 2, 3$ or x, y, z , and the fields \vec{h}, \vec{d} which act on the peripheral spins consist of the external field \vec{H}' and \vec{D}' plus the internal fields. As in II, the fields \vec{h} and \vec{d} are determined self-consistently in terms of \vec{H}', \vec{D}' , and T . We are interested in the limit of zero magnetic fields and consider $\vec{H}' = (0, 0, H')$ let $H' \rightarrow 0^+$ at the end of our calculations. For these fields the magnetic ordering, whenever present, is along the $\alpha = 3$ or z direction and we can let $\vec{h} = (0, 0, h)$. From the definition of the anisotropy field \vec{D}' , see Eq. (38), and for $\vec{H}' = (0, 0, H')$ the quadrupolar ordering is such that we can let $\vec{d} = (d_1, -d_1, d_3)$. Thus, from the equations for self consistency we find the following conditions:

$$(a_+/a_-)^{\gamma} = e^{2h}, \quad (\text{A2a})$$

$$(b_+/b_-)^{\gamma} = e^{2(D'_1 - d_1)}, \quad (\text{A2b})$$

and

$$(b_+ b_- / a_+ a_-)^{\gamma} = e^{2(D'_3 - d_3)}, \quad (\text{A2c})$$

where

$$a_{\pm} \equiv 2 \cosh d_1 + e^{d_3 + \eta' K} \cosh(K \pm h),$$

$$b_{\pm} \equiv e^{\pm d_1} + e^{\mp d_1 + \eta' K} \cosh K + e^{d_3} \cosh h,$$

and

$$\gamma \equiv q - 1.$$

The order parameter $m = \langle S_z \rangle$ for $H' = 0^+$ is found by solving Eqs. (A2) for the internal fields h and \vec{d} . As in Sec. IV we restrict our attention to small values of the quadrupolar pair interaction η' , so that we are sure to have a parallel ordering of the moments and a simultaneous dipolar and quadrupolar phase transition. We determine whether the phase transition is first or second order by finding the sign of the curvature of the order parameter versus temperature plot. When the curvature changes sign the transition is tricritical. To determine the curvature S_k we expand the temperature K and the fields \vec{d} in Eqs. (A2) about the critical point $K_c, \vec{d}_c, h_c = 0$.

$$K(\vec{D}', \eta') = K_c(\vec{D}', \eta') + \frac{1}{2} S_k(\vec{D}', \eta') h^2 + O(h^4), \quad (\text{A3})$$

$$\vec{d}(\vec{D}', \eta') = \vec{d}_c(\vec{D}', \eta') + \frac{1}{2} \vec{S}_d(\vec{D}', \eta') h^2 + O(h^4),$$

where \vec{d} is now a two-dimensional vector $\vec{d} \equiv (d_1, d_3)$.

The tricritical point is defined as

$$S_k(\vec{D}', \eta'_t) = 0. \quad (\text{A4})$$

In the mean-field approximation $\vec{D}'_t = \eta'_t = 0$. As we can vary two fields D'_1 and D'_3 for a fixed value of η' the points satisfying Eq. (A4) form a line. When, in addition, we vary η' , we form surfaces in \vec{D}', η' space on which the phase transition of the model described by Eq. (38) is tricritical.

The determination of $S_k(\vec{D}', \eta')$ for finite \vec{D}' fields and for $\eta' \neq 0$ leads to equations which are more complicated than those encountered in II. Thus, we proceed in the following way. We rewrite the conditions Eqs. (A2) as

$$F_a \equiv a_+ e^{-h/\gamma} - a_- e^{h/\gamma} = 0, \quad (\text{A5a})$$

$$F_b \equiv b_+ - b_- e^{2(D'_1 - d_1)/\gamma} = 0, \quad (\text{A5b})$$

and

$$F_c \equiv b_+ b_- - a_+ a_- e^{2(D'_3 - d_3)/\gamma} = 0. \quad (\text{A5c})$$

Then we expand these functions F_{ν} , $\nu = a, b, c$ about the critical point, $K_c, d_{1c}, d_{3c}, h_c = 0$,

$$F_{\nu} = F_{\nu}|_c + \sum_{\tau} \frac{\partial F_{\nu}}{\partial p_{\tau}} \Big|_c \delta p_{\tau} + \frac{1}{2} \sum_{\tau s} \frac{\partial^2 F_{\nu}}{\partial p_{\tau} \partial p_s} \Big|_c \delta p_{\tau} \delta p_s + \frac{1}{3!} \sum_{\tau s t} \frac{\partial^3 F_{\nu}}{\partial p_{\tau} \partial p_s \partial p_t} \Big|_c \delta p_{\tau} \delta p_s \delta p_t + \dots, \quad (\text{A6})$$

where p_{τ} represents the variables K, d_1, d_3 , and h , δp_{τ} the deviation of the variable from its critical value, and the function and all its derivatives are evaluated at the critical point. Next we use Eqs. (A3) to write the expansion as a power series in the field h ,

$$\delta K = \frac{1}{2} S_k h^2 + O(h^4) \quad (\text{A7})$$

and

$$\delta \vec{d} = \frac{1}{2} \vec{S}_d h^2 + O(h^4).$$

From the definition of the coefficients in Eqs. (A2) we find that the function F_a is an odd function of h while F_b and F_c are even. Therefore when we expand Eq. (A5a) about the critical point the leading terms are linear and cubic in h , while for Eqs. (A5b) and (A5c) the leading terms are a constant and a term quadratic in h . As the functions F_{ν} are zero, the coefficients of the different powers of the field h must vanish. By placing Eqs. (A7) in the expansions Eq. (A6) of the functions Eqs. (A5) and by equating to zero the coefficients of the different powers of h we find the following conditions:

$$\frac{\partial F_a}{\partial h} \Big|_c = 0 = 2e^{d_3 + \eta' K} \sinh K - \frac{2}{\gamma} (2 \cosh d_1 + e^{d_3 + \eta' K} \cosh K), \quad (\text{A8a})$$

$$F_b(K_c, \vec{d}_c, h_c = 0) = 0 = e^{d_3}(1 - e^{2(D'_1 - d_1)/\gamma}), \tag{A8b}$$

$$F_c(K_c, \vec{d}_c, h_c = 0) = 0 = (e^{d_1} + e^{-d_1 + \eta'K} \cosh K + e^{d_3}) \times (e^{-d_1} + e^{d_1 + \eta'K} \cosh K + e^{d_3}) - 2(2 \cosh d_1 + e^{d_3 + \eta'K} \cosh K)^2 e^{2(D'_3 - d_3)/\gamma}, \tag{A8c}$$

$$\sum_r' \frac{\partial^2 F_a}{\partial p_r \partial h} \Big|_c \delta p_r^c = -\left(\frac{1}{3}\right) \frac{\partial^3 F_a}{\partial h^3} \Big|_c, \tag{A9a}$$

$$\sum_r' \frac{\partial F_{\nu'}}{\partial p_r} \Big|_c \delta p_r^c = -\frac{\partial^2 F_{\nu'}}{\partial h^2} \Big|_c, \tag{A9b}$$

where $\nu' = b, c$, the prime on the sum denotes that $p_r = h$ is omitted, and $\delta p_r^c \equiv S_k, \vec{S}_d$, the coefficients of $\frac{1}{2}h^2$ in Eqs. (A7). The three Eqs. (A8) are used to determine the critical temperature $K_c(\vec{D}', \eta')$ and fields $\vec{d}_c(\vec{D}', \eta')$. By placing these solutions in Eqs. (A9) the set of three inhomogeneous equations can be solved for the unknowns δp_r^c , i.e., S_k, S_{d_1} and S_{d_3} . In particular we find

$$S_k(\vec{D}', \eta') = - \frac{\begin{vmatrix} (\frac{1}{3})\partial_h^3 F_a & \partial_{d_1 h}^2 F_a & \partial_{d_3 h}^2 F_a \\ \partial_h^2 F_b & \partial_{d_1} F_b & \partial_{d_3} F_b \\ \partial_h^2 F_c & \partial_{d_1} F_c & \partial_{d_3} F_c \end{vmatrix}}{\begin{vmatrix} \partial_{kh}^2 F_a & \partial_{d_1 h}^2 F_a & \partial_{d_3 h}^2 F_a \\ \partial_k F_b & \partial_{d_1} F_b & \partial_{d_3} F_b \\ \partial_k F_c & \partial_{d_1} F_c & \partial_{d_3} F_c \end{vmatrix}}, \tag{A10}$$

where

$$\begin{aligned} \partial_{kh}^2 F_a &= 2e^{d_3 + \eta'K} [\cosh K - (1/\gamma) \sinh K], \\ \partial_{d_1 h}^2 F_a &= -(4/\gamma) \sinh d_1, \\ \partial_{d_3 h}^2 F_a &= -2e^{d_3 + \eta'K} [(1/\gamma) \cosh K - \sinh K], \\ \partial_h^3 F_a &= -(4/\gamma^3) \cosh d_1 + 2e^{d_3 + \eta'K} [(1 + 3/\gamma^2) \sinh K - (3/\gamma + 1/\gamma^3) \cosh K], \\ \partial_k F_b &= \sinh K e^{\eta'K} (e^{-d_1} - e^{(2D'_1 + (\gamma - 2)d_1)/\gamma}), \\ \partial_{d_1} F_b &= e^{d_1} - e^{-d_1 + \eta'K} \cosh K + [e^{-d_1} - e^{d_1 + \eta'K} \cosh K + (2/\gamma) (e^{-d_1} + e^{d_1 + \eta'K} \cosh K + e^{d_3})] e^{2(D'_1 - d_1)/\gamma}, \\ \partial_{d_3} F_b &= e^{d_3} (1 - e^{2(D'_1 - d_1)/\gamma}), \\ \partial_h^2 F_b &= e^{d_3} (1 - e^{2(D'_1 - d_1)/\gamma}) = \partial_{d_3} F_b, \\ \partial_k F_c &= e^{-d_1 + \eta'K} (\sinh K) (e^{-d_1} + e^{d_1 + \eta'K} \cosh K + e^{d_3}) + e^{d_1 + \eta'K} (\sinh K) \\ &\quad \times (e^{d_1} + e^{-d_1 + \eta'K} \cosh K + e^{d_3}) - 2e^{d_3 + \eta'K} (\sinh K) (2 \cosh d_1 + e^{d_3 + \eta'K} \cosh K) e^{2(D'_3 - d_3)/\gamma}, \\ \partial_{d_1} F_c &= (e^{d_1} - e^{-d_1 + \eta'K} \cosh K) (e^{-d_1} + e^{d_1 + \eta'K} \cosh K + e^{d_3}) - (e^{-d_1} - e^{d_1 + \eta'K} \cosh K) \\ &\quad \times (e^{d_1} + e^{-d_1 + \eta'K} \cosh K + e^{d_3}) - 4(\sinh d_1) (2 \cosh d_1 + e^{d_3 + \eta'K} \cosh K) e^{2(D'_3 - d_3)/\gamma}, \\ \partial_{d_3} F_c &= 2e^{d_3} [(2 \cosh d_1) (1 + e^{\eta'K} \cosh K) + e^{d_3}] - 2[e^{d_3 + \eta'K} (\cosh K) (2 \cosh d_1 + e^{d_3 + \eta'K} \cosh K) \\ &\quad - (2/\gamma) (2 \cosh d_1 + e^{d_3 + \eta'K} \cosh K)^2] e^{2(D'_3 - d_3)/\gamma}, \\ \partial_h^2 F_c &= 2e^{d_3} [(2 \cosh d_1) (1 + e^{\eta'K} \cosh K) + e^{d_3}] - 2e^{d_3 + \eta'K} \\ &\quad \times [(2 \cosh K) (2 \cosh d_1 + e^{d_3 + \eta'K} \cosh K) - (\sinh^2 K) e^{d_3 + \eta'K}] e^{2(D'_3 - d_3)/\gamma} \end{aligned} \tag{A11}$$

and

$$\partial_p F_{\nu'} \equiv \partial F_{\nu'} / \partial p \Big|_c.$$

We have solved Eqs. (A8) for K_c and \vec{d}_c by using the Newton-Raphson technique.⁹ The results are

placed in Eqs. (A10) and (A11) to determine the curvature S_k at the critical point. As the denominator of Eq. (A10) is nonzero, when the numerator is zero the curvature S_k vanishes. Therefore Eq. (A4) which determines the tricritical values for the

anisotropy fields \vec{D}'_i and quadrupolar coupling η'_i is

$$\begin{vmatrix} (\frac{1}{3})\partial_h^3 F_a & \partial_{d_1}^2 F_a & \partial_{d_3}^2 F_a \\ \partial_h^2 F_b & \partial_{d_1} F_b & \partial_{d_3} F_b \\ \partial_h^2 F_c & \partial_{d_1} F_c & \partial_{d_3} F_c \end{vmatrix} = 0. \quad (\text{A12})$$

APPENDIX B: TETRAGONAL STRAINS IN HoSb

By using the BPW approximation to calculate the critical behavior of the cubic model we found that a small anisotropy field is sufficient to drive the system tricritical. For $\eta'=0$, we found $D'_{3t} \cong 0.08$. As $D_1 = 2D'_{3t}kT/\sqrt{3}$, see Eq. (38) and $T_c = 5.4^\circ\text{K}$ for HoSb, we find that the field $D_{1t} = 0.5^\circ\text{K/ion}$ drives the cubic model tricritical. Here we calculate the strain required to produce this anisotropy.

The single-ion magnetoelastic Hamiltonian is given as^{7,10}

$$\mathcal{H}_{\text{me}} = -g_2(\Omega C_\theta^0/N)^{1/2} \epsilon_\theta J^2 (3S_z^2 - 1), \quad (\text{B1})$$

where

$$C_\theta^0 \equiv \frac{1}{2}(C_{11}^0 - C_{12}^0)$$

and

$$\epsilon_\theta \equiv (1/\sqrt{3})(2\epsilon_{zz} - \epsilon_{xx} - \epsilon_{yy}).$$

By comparing \mathcal{H}_{me} with the single-ion anisotropy term in our Hamiltonian Eq. (27) we find that the strain needed to produce an anisotropy field D_1 is

$$\epsilon_\theta = (D_1/2\sqrt{3}) \left[g_2 \left(\frac{C_{11}^0 - C_{12}^0}{2(N/\Omega)} \right)^{1/2} J^2 \right]^{-1}. \quad (\text{B2})$$

For HoSb, $J=8$, and the number of ions per unit volume N/Ω is 1.73×10^{22} ions/cm³. The elastic

constants and the magnetoelastic coupling have been determined by Mullen *et al.*⁷;

$$g_2^2 = 0.11 \times 10^{-3} \text{K/ion}$$

and

$$C_{11}^0 - C_{12}^0 = 13.8 \times 10^{11} \text{ ergs/cm}^3. \quad (\text{B3})$$

By placing these numbers in Eq. (B2), we find the strain required to drive the system tricritical, i.e., to produce $D_1 = D_{1t}$, is

$$\epsilon_{\theta_t} = 4.0 \times 10^{-4}. \quad (\text{B4})$$

This strain is related to the lattice constants a and c as follows¹⁰

$$\epsilon_\theta = (2/\sqrt{3})[(a-c)/a]. \quad (\text{B5})$$

From the x-ray data of Lévy on HoSb¹¹ we find the lattice constant $a = 6.12 \text{ \AA}$. Therefore the difference between the lattice constants a and c necessary to produce the anisotropy field D_{1t} is

$$(a-c)_t = 2 \times 10^{-3} \text{ \AA}. \quad (\text{B6})$$

This difference is within the scatter of experimental values for the lattice constant above the phase transition.¹¹ Therefore it is possible that tetragonal *domains* with $(a-c)$ of the order of $2 \times 10^{-3} \text{ \AA}$ exist above T_c , i.e., in the "cubic" phase, undetected. It is also worth pointing out that the tetragonality $(a-c)$ required for tricriticality is about 10% of the spontaneous tetragonal distortion of the crystal observed at $T = 2.5^\circ\text{K}$, $a-c = 18 \times 10^{-3} \text{ \AA}$. We conclude that it is entirely possible that a nominally cubic crystal as HoSb may be sufficiently strained at low temperature $T \geq 5.4^\circ\text{K}$ for the internal anisotropy fields to drive the first-order phase transition tricritical.

*Research supported in part by the National Science Foundation under Grant No. DMR72-02947.

† Present address: Dept. of Mathematics, University of Melbourne, Parkville, Victoria 3052, Australia.

‡ Address 1975-76: Laboratoire de Physique de Solides, Université de Paris-Sud, Bâtiment 510, 91405 Orsay, France.

¹D. Kim, P. M. Levy, and L. F. Uffer, Phys. Rev. B **12**, 989 (1975); referred to in the text as I.

²D. Kim and P. M. Levy, Phys. Rev. B **12**, 5105 (1975), referred to in text as II.

³G. T. Trammell, Phys. Rev. **131**, 932 (1963).

⁴K. R. Lea, M. J. M. Leask, and W. P. Wolf, J. Phys. Chem. Solids **23**, 1381 (1962).

⁵This behavior has been observed for DySb; see E. Bucher, R. J. Birgeneau, J. P. Maita, G. P. Felcher,

and T. O. Brun, Phys. Rev. Lett. **28**, 746 (1972). One should repeat our calculations for DySb to see whether the coexistence and stability curves nearly overlap for this system.

⁶L. F. Uffer, P. M. Levy, and M. J. Sablik, Solid State Commun. **15**, 191 (1974).

⁷M. E. Mullen, B. Lüthi, P. S. Wang, E. Bucher, L. D. Longinotti, J. P. Maita, and H. R. Ott, Phys. Rev. B **10**, 186 (1974).

⁸See Ref. 6.

⁹B. Carnahan, H. A. Luther, and J. O. Wilkes, *Applied Numerical Methods* (McGraw-Hill, New York, 1970), Secs. 5.8 and 5.9.

¹⁰P. M. Levy, J. Phys. C **6**, 3545 (1973); C **7**, 2760 (1974).

¹¹F. Lévy, Phys. Kondens. Mater. **10**, 85 (1969).